

# Addendum to: Quasiparticle random phase approximation uncertainties and their correlations in the analysis of $0\nu\beta\beta$ decay

Amand Faessler,<sup>1</sup> G.L. Fogli,<sup>2</sup> E. Lisi,<sup>2</sup> V. Rodin,<sup>1,\*</sup> A.M. Rotunno,<sup>3</sup> and F. Šimkovic<sup>4,5</sup>

<sup>1</sup> *Institute of Theoretical Physics, University of Tuebingen, 72076 Tuebingen, Germany*

<sup>2</sup> *Istituto Nazionale di Fisica Nucleare, Sezione di Bari, Via Orabona 4, 70126 Bari, Italy*

<sup>3</sup> *Dipartimento Interateneo di Fisica “Michelangelo Merlin,” Via Amendola 173, 70126 Bari, Italy*

<sup>4</sup> *Department of Nuclear Physics and Biophysics, Comenius University,*

*Mlynská dolina F1, SK-842 15 Bratislava, Slovakia*

<sup>5</sup> *Bogoliubov Laboratory of Theoretical Physics, JINR, 141980 Dubna, Moscow Region, Russia*

In a previous article [Phys. Rev. D **79**, 053001 (2009)] we estimated the correlated uncertainties associated to the nuclear matrix elements (NME) of neutrinoless double beta decay ( $0\nu\beta\beta$ ) within the quasiparticle random phase approximation (QRPA). Such estimates encompass recent independent calculations of NMEs, and can thus still provide a fair representation of the nuclear model uncertainties. In this context, we compare the claim of  $0\nu\beta\beta$  decay in  $^{76}\text{Ge}$  with recent negative results in  $^{136}\text{Xe}$  and in other nuclei, and we infer the lifetime ranges allowed or excluded at 90% C.L. We also highlight some issues that should be addressed in order to properly compare and combine results coming from different  $0\nu\beta\beta$  candidate nuclei.

PACS numbers: 23.40.-s, 21.60.Jz, 02.50.-r

## I. INTRODUCTION

In a previous paper [1] we presented the results of a systematic evaluation of nuclear matrix elements (NME) and of their correlated uncertainties for the neutrinoless double beta decay process ( $0\nu\beta\beta$ ) in different nuclei, within the quasiparticle random phase approximation (QRPA) and the standard framework of light Majorana neutrinos with effective mass  $m_{\beta\beta}$ . In particular, in [1] we discussed in the joint statistical distribution of the NME values  $|M'_i|$  which govern, together with the phase space  $G_i$ , the decay half life  $T_i$  in the  $i$ -th candidate nucleus,

$$T_i^{-1} = G_i |M'_i|^2 m_{\beta\beta}^2, \quad (1)$$

with  $i$  spanning the set

$$i = {}^{76}\text{Ge}, {}^{82}\text{Se}, {}^{96}\text{Zr}, {}^{100}\text{Mo}, {}^{116}\text{Cd}, {}^{128}\text{Te}, {}^{130}\text{Te}, {}^{136}\text{Xe}. \quad (2)$$

We emphasized that the correlations among the NME uncertainties are sizable and play a relevant role in comparing  $0\nu\beta\beta$  data from different nuclei, including the  $^{76}\text{Ge}$  decay events claimed by Klapdor *et al.* in [2, 3].

Recently, important new limits on the  $^{136}\text{Xe}$  half life have been obtained by the experiments EXO-200 [4] and KamLAND-Zen [5], which have reached, for various choices of NME calculations, a 90% C.L. sensitivity to  $m_{\beta\beta}$  largely overlapping with the  $m_{\beta\beta}$  range favored by the  $^{76}\text{Ge}$  claim [4, 5]. These advances have prompted us to use the results in [1] to perform a systematic comparison of  $^{136}\text{Xe}$  half-life limits with those obtained in other nuclei and with the  $^{76}\text{Ge}$  claim. The comparison is worked out in detail in the next Section, in terms of half-life ranges allowed or excluded at 90% C.L. Once more, NME covariances are shown to play a relevant role in the  $0\nu\beta\beta$  phenomenology. We also point out that, in order to fully exploit the implications of upcoming  $0\nu\beta\beta$  results, it is generally advisable to discuss in some detail the probability distributions of both the experimental half lives and the theoretical NMEs.

We remark that, in this Addendum to [1], we adopt the same NME and covariances as computed therein. A systematic update of [1] would require extensive QRPA calculations of hundreds of NME, which are left to a future study. However, as we argue in the Appendix, the uncertainties in [1] are conservative enough to embrace recent NME calculations, using either the QRPA or independent theoretical frameworks. We conclude that the NME estimates in [1] still provide a fair representation of the current spread of theoretical  $0\nu\beta\beta$  calculations.

---

\*Now at Stuttgart Technology Center, Sony Deutschland GmbH, Hedelfinger Strasse 61, D-70327 Stuttgart, Germany.

## II. COMPARISON OF THE $0\nu\beta\beta$ CLAIM WITH RECENT RESULTS

In this section we briefly review, for the sake of completeness, the notation and conventions used in [1] and the implications of the  $0\nu\beta\beta$  claim in  $^{76}\text{Ge}$  for different nuclei. Then we compare such implications with recent experimental data, most notably from  $^{136}\text{Xe}$  in EXO-200 and KamLAND-Zen, and discuss the regions allowed or excluded at 90% C.L. We remind that gaussian uncertainties at  $n$  standard deviations on a given parameter correspond to projections of  $\Delta\chi^2 = n^2$  regions on that parameter, and that 90% C.L. uncertainties correspond to  $n = 1.64$ .

### A. Notation, conventions, and implications of $^{76}\text{Ge}$ $0\nu\beta\beta$ claim

As in [1], we linearize Eq. (1) as

$$\tau_i = \gamma_i - 2\eta_i - 2\mu, \quad (3)$$

by taking logarithms of the relevant  $0\nu\beta\beta$  quantities in appropriate units:

$$\tau_i = \log_{10}(T_i/\text{y}), \quad (4)$$

$$-\gamma_i = \log_{10}[G_i/(\text{y}^{-1}\text{eV}^{-2})], \quad (5)$$

$$\eta_i = \log_{10}|M'_i|, \quad (6)$$

$$\mu = \log_{10}(m_{\beta\beta}/\text{eV}). \quad (7)$$

The NME central values with their one-standard-deviation errors are denoted as

$$\eta_i = \eta_i^0 \pm \sigma_i, \quad (8)$$

where the  $\sigma_i$  are positively correlated through a matrix  $\rho_{ij}$ . Table I in [1] reports the numerical values of  $\gamma_i$ ,  $\eta_i^0$ ,  $\sigma_i$ , and  $\rho_{ij}$ , which are adopted hereafter.

Let us assume that  $0\nu\beta\beta$  decay has been experimentally observed in  $i = ^{76}\text{Ge}$  as claimed by Klapdor *et al.* [2, 3], with (logarithmic) half life given at  $\pm 1\sigma$  as [1]:

$$\tau_i = \tau_i^0 \pm s_i \quad (9)$$

$$= 25.355 \pm 0.072 \text{ (} i = ^{76}\text{Ge) } . \quad (10)$$

Then, Eq. (3) predicts the following half life in a different nucleus  $j \neq i$  [1]

$$\tau_j = \tau_j^0 \pm s_j, \quad (11)$$

where

$$\tau_j^0 = \tau_i^0 + (\gamma_j - \gamma_i) - 2(\eta_j^0 - \eta_i^0), \quad (12)$$

and

$$s_j^2 = s_i^2 + 4(\sigma_i^2 + \sigma_j^2 - 2\rho_{ij}\sigma_i\sigma_j), \quad (13)$$

the  $(s_i, s_j)$  correlation being given by [1]

$$r_{ij} = \frac{s_i}{s_j} \text{ (} i \neq j \text{) } . \quad (14)$$

We add here that, for two nuclei  $j$  and  $k$  different from  $i = ^{76}\text{Ge}$ , the  $(s_j, s_k)$  correlation is given by

$$r_{jk} = \frac{s_j^2 + s_k^2 - 4(\sigma_j^2 + \sigma_k^2 - 2\rho_{jk}\sigma_j\sigma_k)}{2s_js_k} \text{ (} j \neq i \neq k \text{) } , \quad (15)$$

see also the Appendix.

TABLE I: Best current limits on half-lives at 90% C.L. ( $T_j > T_j^{90}$  and  $\tau_j > \tau_j^{90}$ ) for different nuclei  $j$ .

$j$	$T_j^{90}/\text{y}$	$\tau_j^{90}$	Experiment	Ref.
$^{76}\text{Ge}$	$1.6 \times 10^{25}$	25.204	IGEX	[6]
$^{82}\text{Se}$	$3.6 \times 10^{23}$	23.556	NEMO-3	[7]
$^{96}\text{Zr}$	$9.2 \times 10^{21}$	21.964	NEMO-3	[7]
$^{100}\text{Mo}$	$1.1 \times 10^{24}$	24.041	NEMO-3	[7]
$^{116}\text{Cd}$	$1.7 \times 10^{23}$	23.230	Solotvina	[8]
$^{128}\text{Te}$	$7.7 \times 10^{24}$	24.886	Geochem.	[9]
$^{130}\text{Te}$	$2.8 \times 10^{24}$	24.447	CUORICINO	[10]
$^{136}\text{Xe}$	$3.4 \times 10^{25}$	25.531	EXO $\oplus$ KL-Zen	[4, 5]

### B. Applications and comparison with recent data

Except for the claim in [2, 3], all other  $0\nu\beta\beta$  experiments report negative results to date. Table I shows the current best limits at 90% C.L. on the  $0\nu\beta\beta$  half life in different nuclei  $j$  (i.e.,  $T_j^{90}$  and its logarithm  $\tau_j^{90}$ ). Particularly important are the recent limits on  $^{136}\text{Xe}$  coming from EXO-200 ( $T^{90} = 1.6 \times 10^{25}$  y) [4] and from KamLAND-Zen ( $T^{90} = 1.9 \times 10^{25}$  y). A statistical combination of the negative results in [4, 5] is attempted in Ref. [5], where the combined “EXO  $\oplus$  KL-Zen” limit  $T^{90}(^{136}\text{Xe}) = 3.4 \times 10^{25}$  y is quoted, as reported in Table I and adopted hereafter.

Figure 1 shows the limits reported in Table I (one-sided bands), together with the 90% C.L. ranges implied by the  $^{76}\text{Ge}$  claim, as derived from Eqs. (10)–(13) with errors inflated by  $\times 1.64$ . It can be seen that, for the first time, there is a significant overlap between the half-life limit in one nucleus ( $^{136}\text{Xe}$ ) and the corresponding region favored by Klapdor’s claim for a given set of NME, as also emphasized in the experimental papers [4, 5]. This situation should be contrasted with the analogous Fig. 5 in [1], where no overlap emerged.

In principle, the next logical step should be a combination of positive and negative  $0\nu\beta\beta$  results—within the adopted set of NME and their covariances—in order to evaluate the statistical consistency of the data (test of hypothesis) and to identify the range of  $m_{\beta\beta}$  consistent with all the results (parameter estimation). This task would require the detailed knowledge of the probability distribution functions, not only for the NME (as attempted in [1]), but also for the  $^{76}\text{Ge}$  and  $^{136}\text{Xe}$  half lives. However, the half-life likelihoods have not been published in the original papers [2, 3] and [4, 5]. Reproducing or simulating the original data analyses is difficult, especially for the claimed signal in  $^{76}\text{Ge}$ , which involved a dedicated pulse-shape discrimination [3]. It would be desirable that future  $0\nu\beta\beta$  results are published also in terms of likelihood or  $\chi^2$  functions of the half-life, and not only in terms of specific bounds, say, at 90% C.L. Concerning theoretical uncertainties, we also note that after [1] there has been no other independent study of NME error correlations from the viewpoint of different nuclear models. Therefore, we think that the conditions for a quantitative combination or a “global fit” of positive and negative  $0\nu\beta\beta$  results are currently not warranted.

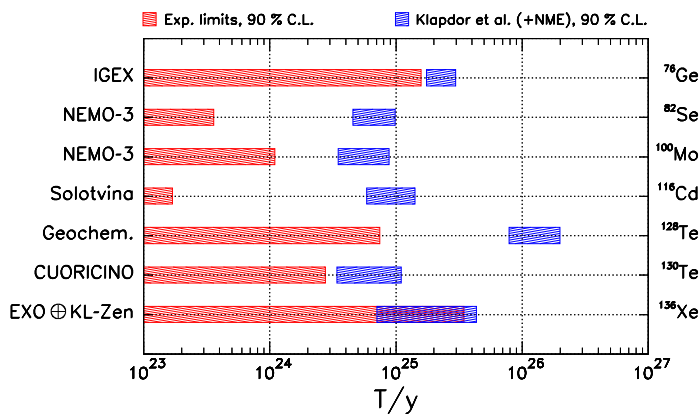


FIG. 1: Range of half lives  $T_i$  preferred at 90% C.L. by the  $0\nu\beta\beta$  claim of [3], compared with the 90% exclusion limits placed by other experiments. The comparison involves the NME and their errors, as well as their correlations. Note the overlap of favored and disfavored ranges for  $^{136}\text{Xe}$ . This figure updates Fig. 5 of [1].

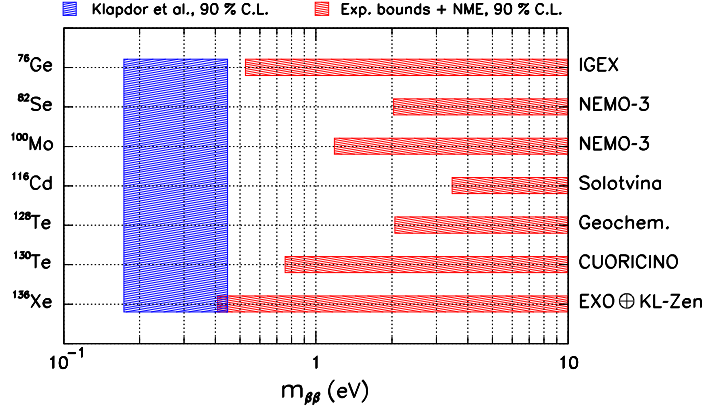


FIG. 2: Range of  $m_{\beta\beta}$  allowed by the  $0\nu\beta\beta$  claim of [3], compared with the limits placed by other experiments (all at 90% C.L.). This figure updates Fig. 3 of [1].

The above issues emerge, e.g., when one tries to translate the numbers in Table I and Eq. (10) in terms of 90% C.L. limits on  $m_{\beta\beta}$  via Eq. (3). In the absence of the experimental likelihood functions for the half lives, the combination of one-sided experimental limits ( $\tau^{90}$ ) with two-sided theoretical errors ( $\pm 1.64\sigma_i$ ) is not obvious. Conservatively, one may combine linearly the experimental and theoretical ranges at 90% C.L. as proposed in [1], at the price of losing statistical power. Figure 2 shows the results of such combination, in terms of favored and disfavored ranges of  $m_{\beta\beta}$ . It can be noticed that the  $^{136}\text{Xe}$  limits overlap with the range favored by the  $^{76}\text{Ge}$  claim, but not as much as in Fig. 1, signaling the loss of statistical information. Therefore, we prefer to show the following results directly in terms of the observable half lives  $T_i$  and not via  $m_{\beta\beta}$ .

Figure 3 shows the application of Eqs. (10)–(14) in the plane charted by the half lives ( $T_i, T_j$ ) for  $i = ^{76}\text{Ge}$  and  $j = ^{136}\text{Xe}$ , at 90% C.L. The horizontal band corresponds to Klapdor’s claim, while the slanted band represents the theoretical range at the  $\pm 1.64\sigma$  level [1]. Their combination provides the allowed ellipse, which is however largely disfavored by the one-sided limit placed by EXO  $\oplus$  KL-Zen (vertical bound). The surviving ellipse segment corresponds to  $T(^{76}\text{Ge}) \simeq 2.0\text{--}2.9 \times 10^{25}$  y and  $T(^{136}\text{Xe}) \simeq 3.4\text{--}4.3 \times 10^{25}$  y. The upper ends of such ranges set the limits required to test Klapdor’s claim at 90% C.L. Such an exercise could be repeated at higher C.L., if the corresponding experimental limits or the half-life likelihood were also published; this will become important in the future, since the  $\sim 6\sigma$  signal claimed by Klapdor *et al.* [2, 3] should be tested at C.L. definitely higher than 90%.

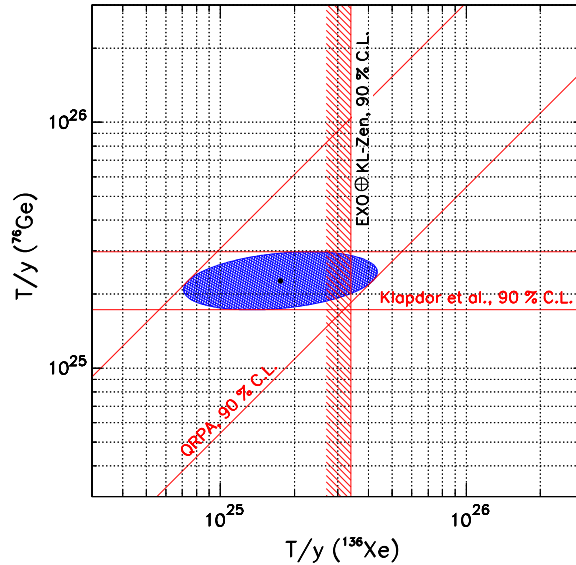


FIG. 3: Theoretical and experimental constraints in the plane charted by the  $0\nu\beta\beta$  half-lives of  $^{76}\text{Ge}$  and  $^{136}\text{Xe}$ . Horizontal band: range preferred by the  $0\nu\beta\beta$  claim of [3]. Slanted band: constraint placed by our QRPA estimates [1]. The combination provides the shaded ellipse, whose projection on the abscissa gives the range preferred at 90% C.L. for the  $^{136}\text{Xe}$  half life. This range is largely disfavored by the combined EXO  $\oplus$  KL-Zen results [4, 5] (vertical one-sided limit).

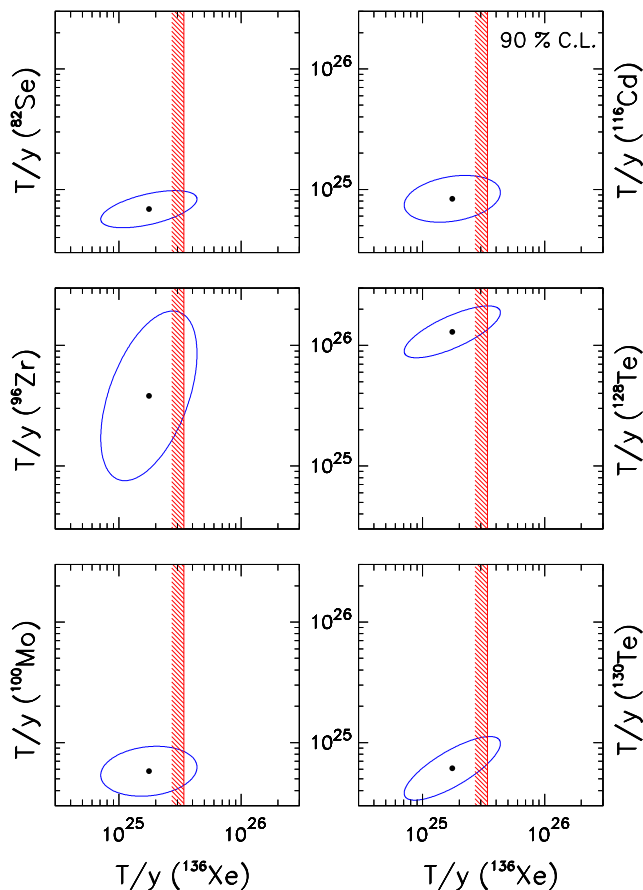


FIG. 4: Allowed regions (ellipses) as derived from Klapdor’s claim [3] and the NME of [1], in the plane charted by the half lives of  $^{136}\text{Xe}$  and each of the six nuclei  $^{82}\text{Se}$ ,  $^{96}\text{Zr}$ ,  $^{100}\text{Mo}$ ,  $^{116}\text{Cd}$ ,  $^{128}\text{Te}$ , and  $^{130}\text{Te}$ . A large fraction of each ellipse is excluded by the combined EXO  $\oplus$  KL-Zen results [4, 5] (vertical one-sided limit). All bounds are at 90% C.L. on one variable.

Figure 4 shows the application of Eqs. (13) and (15) in the six planes charted by the half lives ( $T_j, T_k$ ) for  $j = ^{136}\text{Xe}$  and  $k \neq ^{136}\text{Xe}, ^{76}\text{Ge}$ . In each panel, the ellipse represents the region favored by Klapdor’s claim within the adopted NME and their covariances, to be compared with the region excluded by EXO  $\oplus$  KL-Zen at the same C.L. (vertical bound). As a consequence of the positive correlation, the ellipse segment not excluded by the  $^{136}\text{Xe}$  limit corresponds, for each  $k$ -th nucleus, to the higher end of the half-life range at 90% C.L. For instance, in the case of  $^{130}\text{Te}$  (lower right panel in Fig. 4), the current limit should be pushed from  $2.8 \times 10^{24}$  y up to  $\sim 0.7\text{--}1.1 \times 10^{25}$  y, in order to cover the ellipse segment left out by the current EXO  $\oplus$  KL-Zen bound. If correlations were neglected, the ellipse would not be tilted, and this requirement would (incorrectly) become less stringent.

We remark that the results shown in this section are based on the same NME and covariances as in [1]. In general, it would be useful to extend the theoretical covariance analysis in further directions, including: (i) updated and improved QRPA calculations; (ii) other candidate  $0\nu\beta\beta$  nuclei not considered in [1]; (iii) theoretical NME approaches different from the QRPA (see also the Appendix); (iv) nonstandard decay mechanisms. From the experimental viewpoint, we have emphasized the importance of publishing the probability distribution of the half life for each nucleus. All these refinements will become increasingly important in the next few years, since a number of  $0\nu\beta\beta$  experiments will provide highly significant data, which must be eventually combined in proper theoretical and statistical frameworks.

### III. SUMMARY

In the previous work [1] we presented estimates of NME and their covariances for a set of candidate  $0\nu\beta\beta$  nuclei, within the QRPA theoretical framework. Such estimates still provide a fair representation of the spread of NME calculations (see the Appendix). In this context, we have compared herein the claimed  $^{76}\text{Ge}$  signal from [2, 3] with negative results from other experiments, including the recent  $^{136}\text{Xe}$  limits placed by EXO-200 [4] and KamLAND-Zen [5]. We have worked out favored and disfavored ranges at 90% C.L. for each nucleus and for couples of nuclei, in

terms of either half lives  $T_j$  (Figs. 1, 3 and 4) or of  $m_{\beta\beta}$  (Fig. 2). In particular, we find that, in order to close the region currently allowed at 90% C.L. by the  $^{76}\text{Ge}$  claim and by the  $^{136}\text{Xe}$  limit, one should cover either the range  $T(^{76}\text{Ge}) \simeq 2.0\text{--}2.9 \times 10^{25}$  y or the range  $T(^{136}\text{Xe}) \simeq 3.4\text{--}4.3 \times 10^{25}$  y; alternatively, using a third nucleus such as  $^{130}\text{Te}$ , one should cover the range  $T(^{130}\text{Te}) \simeq 0.7\text{--}1.1 \times 10^{25}$  y (see also Fig. 4 for other nuclei). We remark that the theoretical NME covariances play a relevant role in these or similar estimates: their study should thus be further pursued, not only within the QRPA [1], but also within other approaches as well as for nonstandard  $0\nu\beta\beta$  mechanisms. We have also emphasized that experimental results should be given in terms of likelihood functions for the decay half-life (rather than in terms of bounds at a fixed C.L.), in order to allow a proper combination of the experimental and theoretical uncertainties, which are equally important to derive constraints on  $0\nu\beta\beta$  parameters.

*Acknowledgments.* The work of G.L.F., E.L., and A.M.R. is supported by the Italian Istituto Nazionale di Fisica Nucleare (INFN) and Ministero dell’Istruzione, dell’Università e della Ricerca (MIUR) through the “Astroparticle Physics” project. F.Š. is supported by the VEGA Grant Agency of the Slovak Republic under contract N. 1/0876/12.

## APPENDIX

In the Appendix of Ref. [1], we clarified the role of different conventions about the phase space factors  $G_i$  and the nuclear matrix elements  $|M'_i|$ . We also compared our QRPA estimates for the NME logarithms  $\eta_i$  with those calculated independently in [11] (within the QRPA) and in [12, 13] (within the shell model, SM), which were all encompassed by our  $\pm 3\sigma$  ranges ( $\eta_i^0 \pm 3\sigma_i$ ). In this Appendix, we show that such ranges also embrace more recent NME calculations performed via the Energy Density Functional method (EDF) [14], the microscopic Interacting Boson Model (IBM-2) [15], and the projected Hartree-Fock-Bogoliubov method (PHFB) [16], as well as the Renormalized QRPA (RQRPA) approach [17]. The last calculation is particularly relevant with respect to [1], since it embeds the recent experimental determination of the  $2\nu 2\beta$  half life in  $^{136}\text{Xe}$  [18, 19] (not available at the time of [1]), which fixes the so-called  $g_{pp}$  parameter of the QRPA.

Different NME calculations may use slightly different phase space factors (see the recent detailed evaluation in [20]), different values of the nuclear radius parameter  $r_0$ , and different conventions. In order to make a homogeneous comparison with the  $\eta$  values and the conventions of [1], we use the fact that the papers [14–17] contain tables of estimated half lives ( $\tau_i$ ) at fixed values of the effective Majorana mass ( $\mu$ ); then, by adopting the same phase space factor ( $\gamma_i$ ) reported in [1], the NME values ( $\eta_i$ ) can be calculated via Eq. (3) and can be directly compared with those in [1]. For this purpose, we use the half lives in Table I of [14], in Table III of [15], in Table IV of [16] (central values), and in Table I of [17] (central values). From [17] we select two options, RQRPA with Jastrow short-range correlations, and QRPA with CD-Bonn potential, which generally provide the lowest and highest NME values, respectively [17]. We note that the papers [16, 17] also report estimated NME uncertainties, but not their covariance matrix; in any case, the errors estimated in [1] are generally more conservative than those in [16, 17].

Table II reports the effective  $\eta_i$  of such recent EDF, IBM-2, PHFB, and (R)QRPA calculations, to be compared with the  $\pm 3\sigma$  ranges from [1] in the last two rows. Such ranges largely embrace all the above values. Actually, almost all the NME in Table II are contained in the 90% C.L. ranges ( $\eta_i^0 \pm 1.64\sigma_i$ , not shown). We conclude that Table I of [1] still provide a reasonable and conservative evaluation of the NME  $\eta_i$  and of their variances  $\sigma_i^2 = \text{var}(\eta_i)$ .

TABLE II: Estimates of  $\eta_i = \log_{10} |M'_i|$  for each nucleus, as derived from the recent EDF [14], IBM-2 [15], and PHFB [16] calculations after appropriate rescaling, in order to match the conventions used in [1]. The estimates of [16] refer only to a subset of nuclei. Also shown are the  $\eta_i$  central values for two widely different (R)QRPA models recently reported in [17]. The corresponding values of the adopted effective axial coupling  $g_A$  are also reported. The last two rows report the upper and lower ends of our  $3\sigma$  range  $\eta_i^0 \pm 3\sigma_i$  as taken from [1], which largely encompass the above  $\eta_i$  values.

Ref.	Model	$g_A$	$^{76}\text{Ge}$	$^{82}\text{Se}$	$^{96}\text{Zr}$	$^{100}\text{Mo}$	$^{116}\text{Cd}$	$^{128}\text{Te}$	$^{130}\text{Te}$	$^{136}\text{Xe}$
[14]	EDF	$1.25 \times 0.74$	0.617	0.577	0.707	0.663	0.629	0.570	0.665	0.571
[15]	IBM-2	1.269	0.721	0.622	0.390	0.564	0.421	0.616	0.562	0.467
[16]	PHFB	1.254			0.474	0.813		0.586	0.623	
[16]	PHFB	1.0			0.317	0.658		0.433	0.470	
[17]	RQRPA (Jastrow)	1.0	0.535	0.460	0.045	0.365	0.289	0.401	0.291	0.160
[17]	QRPA (CD-Bonn)	1.25	0.797	0.748	0.316	0.717	0.597	0.736	0.689	0.468
[1]	Lower limit of our $3\sigma$ range		0.269	0.166	−0.703	0.017	−0.046	0.072	0.024	−0.307
[1]	Upper limit of our $3\sigma$ range		1.001	0.976	0.779	0.989	0.854	0.996	0.972	0.815

Concerning the NME covariances,  $\text{cov}(\eta_i, \eta_j) = \rho_{ij}\sigma_i\sigma_j$ , no comparison is possible within the current literature, since they have been evaluated only in [1]. Here we just remind their crucial role, by deriving the last three equations in Sec. II A. Since the experimental error  $s_i$  ( $i = {}^{76}\text{Ge}$ ) in Eq. (10) is independent from any theoretical error  $\sigma_j$ , it is  $\text{cov}(\tau_i, \eta_j) = 0$ ; in addition, phase space uncertainties are currently negligible,  $\text{var}(\gamma_j) \simeq 0$ . Thus, in the nontrivial case  $j \neq i$ , propagation of errors in Eq. (12) gives

$$\begin{aligned} s_j^2 &\equiv \text{var}(\tau_j) \\ &= \text{var}(\tau_i) + 4[\text{var}(\eta_j) + \text{var}(\eta_i) - 2\text{cov}(\eta_i, \eta_j)] \\ &= s_i^2 + 4(\sigma_i^2 + \sigma_j^2 - 2\rho_{ij}\sigma_i\sigma_j) \end{aligned} \quad (16)$$

and

$$\begin{aligned} r_{ij}s_i s_j &\equiv \text{cov}(\tau_i, \tau_j) \\ &= \text{cov}(\tau_i, \tau_i) \\ &= s_i^2, \end{aligned} \quad (17)$$

as reported in Eqs. (13) and (14). Similarly, for  $j \neq i$  and  $k \neq i$  (where  $i = {}^{76}\text{Ge}$ ), it is

$$\begin{aligned} r_{jk}s_j s_k &\equiv \text{cov}(\tau_j, \tau_k) \\ &= \text{cov}(\tau_i, \tau_i) + 4\text{cov}(\eta_i, \eta_i) - 4\text{cov}(\eta_i, \eta_k) - 4\text{cov}(\eta_i, \eta_j) + 4\text{cov}(\eta_j, \eta_k) \\ &= s_i^2 + 4\sigma_i^2 - 4\rho_{ij}\sigma_i\sigma_j - 4\rho_{ik}\sigma_i\sigma_k + 4\rho_{jk}\sigma_j\sigma_k \\ &= \frac{1}{2}(s_j^2 + s_k^2) - 2(\sigma_j^2 + \sigma_k^2 - 2\rho_{jk}\sigma_j\sigma_k), \end{aligned} \quad (18)$$

as reported in Eq. (15). The relevance of NME covariances clearly emerges in the above equations.

- 
- [1] A. Faessler, G. L. Fogli, E. Lisi, V. Rodin, A. M. Rotunno and F. Šimkovic, “Quasiparticle random phase approximation uncertainties and their correlations in the analysis of  $0\nu\beta\beta$  decay,” *Phys. Rev. D* **79**, 053001 (2009) [arXiv:0810.5733 [hep-ph]].
  - [2] H. V. Klapdor-Kleingrothaus, I. V. Krivosheina, A. Dietz and O. Chkvorets, “Search for neutrinoless double beta decay with enriched Ge-76 in Gran Sasso 1990-2003,” *Phys. Lett. B* **586**, 198 (2004) [arXiv:hep-ph/0404088].
  - [3] H. V. Klapdor-Kleingrothaus and I. V. Krivosheina, “The Evidence For The Observation Of  $0\nu\beta\beta$  Decay: The Identification Of  $0\nu\beta\beta$  Events From The Full Spectra,” *Mod. Phys. Lett. A* **21**, 1547 (2006).
  - [4] M. Auger *et al.* [EXO Collaboration], “Search for Neutrinoless Double-Beta Decay in  ${}^{136}\text{Xe}$  with EXO-200,” *Phys. Rev. Lett.* **109**, 032505 (2012) [arXiv:1205.5608 [hep-ex]].
  - [5] A. Gando *et al.* [KamLAND-Zen Collaboration], “Limit on Neutrinoless  $\beta\beta$  Decay of Xe-136 from the First Phase of KamLAND-Zen and Comparison with the Positive Claim in Ge-76,” arXiv:1211.3863 [hep-ex].
  - [6] C. E. Aalseth *et al.* [IGEX Collaboration], “The IGEX Ge-76 neutrinoless double-beta decay experiment: Prospects for next generation experiments,” *Phys. Rev. D* **65**, 092007 (2002) [arXiv:hep-ex/0202026].
  - [7] A. S. Barabash, talk at *NPAE 2012*, 4th International Conference on Current Problems in Nuclear Physics and Atomic Energy (Kyiv, Ukraine, 2012): “Double beta decay experiments: Beginning of a new era,” arXiv:1209.4241 [nucl-ex].
  - [8] F. A. Danevich *et al.*, “Search for double beta decay of cadmium and tungsten isotopes: Final results of the Solotvina experiment,” *Phys. Rev. C* **68**, 035501 (2003).
  - [9] T. Bernatowicz, J. Brannon, R. Brazzle, R. Cowsik, C. Hohenberg and F. Podosek, “Precise determination of relative and absolute  $\beta\beta$  decay rates of  ${}^{128}\text{Te}$  and  ${}^{130}\text{Te}$ ,” *Phys. Rev. C* **47**, 806 (1993).
  - [10] E. Andreotti *et al.*, “ ${}^{130}\text{Te}$  Neutrinoless Double-Beta Decay with CUORICINO,” *Astropart. Phys.* **34**, 822 (2011) [arXiv:1012.3266 [nucl-ex]].
  - [11] J. Suhonen and M. Kortelainen, “Nuclear matrix elements for double beta decay,” *Int. J. Mod. Phys. E* **17**, 1 (2008).
  - [12] J. Menendez, A. Poves, E. Caurier and F. Nowacki, “Disassembling the Nuclear Matrix Elements of the Neutrinoless  $\beta\beta$  Decay,” *Nucl. Phys. A* **818**, 139 (2009) [arXiv:0801.3760 [nucl-th]].
  - [13] J. Menendez, A. Poves, E. Caurier and F. Nowacki, “Deformation and the Nuclear Matrix Elements of the Neutrinoless Double Beta Decay,” arXiv:0809.2183 [nucl-th].
  - [14] T. R. Rodriguez and G. Martinez-Pinedo, “Energy density functional study of nuclear matrix elements for neutrinoless  $\beta\beta$  decay,” *Phys. Rev. Lett.* **105**, 252503 (2010) [arXiv:1008.5260 [nucl-th]].
  - [15] J. Barea, J. Kotila and F. Iachello, “Limits on Neutrino Masses from Neutrinoless Double-beta Decay,” *Phys. Rev. Lett.* **109**, 042501 (2012).
  - [16] P. K. Rath, R. Chandra, K. Chaturvedi, P. K. Raina and J. G. Hirsch, “Uncertainties in nuclear transition matrix elements for neutrinoless  $\beta\beta$  decay within the PHFB model,” *Phys. Rev. C* **82**, 064310 (2010) [arXiv:1104.3965 [nucl-th]].

- [17] A. Faessler, V. Rodin and F. Simkovic, “Nuclear matrix elements for neutrinoless double-beta decay and double-electron capture,” *J. Phys. G* **39**, 124006 (2012) [arXiv:1206.0464 [nucl-th]].
- [18] N. Ackerman *et al.* [EXO-200 Collaboration], “Observation of Two-Neutrino Double-Beta Decay in  $^{136}\text{Xe}$  with EXO-200,” *Phys. Rev. Lett.* **107**, 212501 (2011) [arXiv:1108.4193 [nucl-ex]].
- [19] A. Gando *et al.* [KamLAND-Zen Collaboration], “First result from KamLAND-Zen : Double beta decay with  $^{136}\text{Xe}$ ,” arXiv:1205.6130 [hep-ex].
- [20] J. Kotila and F. Iachello, “Phase space factors for double- $\beta$  decay,” *Phys. Rev. C* **85**, 034316 (2012) [arXiv:1209.5722 [nucl-th]].